Step Size Bound for Narrowband Feedback Active Noise Control

Liang Wang[1], Woon-Seng Gan[2], Yong-Kim Chong[2], Sen M Kuo[3]
[1]DTS Inc, Singapore;
[2]School of Electrical and Electronic Engineering, Nanyang Technological University, Singapore
[3]Department of Electrical Engineering, Northern Illinois University, USA
[1]E-mail: Vincent.Wang@dts.com
[2]E-mail: ewsgan@ntu.edu.sg
[3]E-mail: kuo1065@gmail.com

***Abstract*— This paper presents the derivation of the convergence analysis of the feedback active noise control under perfect and imperfect secondary path transfer functions. Existing analysis approaches do not include the analysis of the reference signal synthesis errors due to the complexity of interrelated feedback nature. A detailed derivation of the maximum step size bound for the feedback active noise control system has been formulated for perfect and imperfect secondary-path estimation. This theoretical work has been verified by computer simulations.**

I. INTRODUCTION

Active noise control (ANC) [1] is achieved by introducing a canceling "anti-noise" though a secondary source. The secondary source is connected through an electronic system using a specific signal processing algorithm for the particular cancellation scheme. ANC is an effective way to attenuate low-frequency noise that is very difficult or expensive to control using passive means.

There are two commonly used ANC structures, namely feedforward and feedback ANC systems. The difference between these systems lie in the presence of reference sensor (can be either a microphone or non-acoustical sensors) in the feedforward ANC system; whereas, the feedback ANC synthesizes a reference signal based on the measured error signal and the estimated secondary path. Figures 1 and 2 show the block diagrams of the feedforward and feedback ANC system, respectively. Notice that the reference signal, $x(n)$ is acquired in the feedforward ANC system, while it is synthesized in the feedback ANC system. The adaptive algorithm used in updating the filter coefficients, $W(z)$ is the commonly used filtered-x least-mean-square (FXLMS) algorithm [2-4]. In some applications, it is difficult or may not be possible to mount the reference sensors close to the noise source. These difficulties in using reference sensors promote the application of the feedback ANC system, which does not require any reference input. However, the noise canceling performance of the feedback ANC system is usually limited compared to the feedforward ANC system. For example, the bandwidth of noise that can be cancelled in feedback ANC system is usually narrower than that of the feedforward ANC system.

The convergence of the feedback ANC system was mostly examined only under perfect secondary path estimation[5-6]. In this paper, we briefly examine the convergence analysis of the feedback ANC system under both perfect and imperfect secondary path. A more detailed description with more results will be reported in a journal paper submitted by the authors [7].

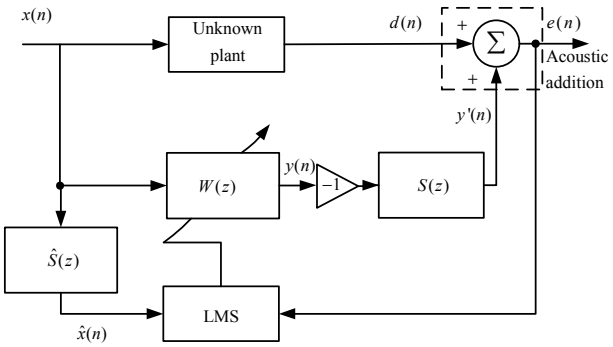

Figure 1: Feedforward ANC System

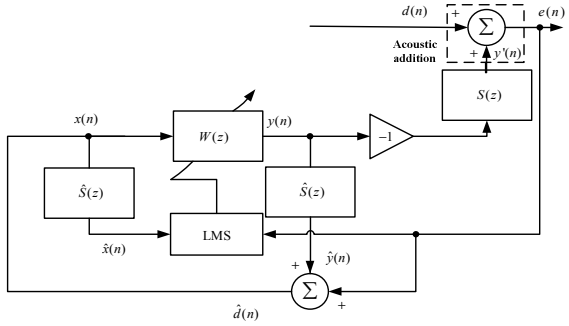

Figure 2: Feedback ANC System

In the feedback ANC system, one of the main task is to synthesize the reference signal $\hat{d}(n)$ using the measured error signal and the estimated secondary-path given by

$$\begin{aligned} x(n) &\equiv \hat{d}(n) \\ &= e(n) + \hat{\mathbf{s}}^T(n)\mathbf{y}(n), \end{aligned} \tag{1}$$

where $e(n)$ is the error signal picked up by the error sensor and $\hat{\mathbf{s}}(n) = [\hat{s}_1(n),\ \hat{s}_2(n),\ \ldots\ \hat{s}_{L_s}(n)]^T$ is the impulse response vector of the estimated secondary-path with length L_s. The secondary signal vector $\mathbf{y}(n)$, which is the anti-noise, is obtained by convolution between the weight vector $\mathbf{w}(n) = \left[w_0(n), w_1(n), \cdots, w_L(n)\right]^T$ at time n and the synthesized reference signal, as follows:

$$y(n) = \mathbf{w}^T(n)\mathbf{x}(n). \tag{2}$$

The L adaptive filter coefficients of the weight vector is updated by the following FXLMS algorithm:

$$\mathbf{w}(n+1) = \mathbf{w}(n) + \mu\hat{\mathbf{x}}(n)e(n), \tag{3}$$

where μ is the step size that determines stability and convergence rate of the algorithm, and $\hat{\mathbf{x}}(n) = [\hat{x}(n), \hat{x}(n-1), \ldots \hat{x}(n-L+1)]^T$ is the filtered reference (or filtered-x) signal vector, where

$$\hat{x}(n) = \sum_{j=1}^{L_s} \hat{s}_j(n)x(n-j+1). \tag{4}$$

As shown in Figure 2, the signal $\hat{y}(n)$, which is the filtered (by estimated secondary path) output signal, is written as

$$\hat{y}(n) = \hat{\mathbf{s}}^{\mathrm{T}}(n)\mathbf{y}(n). \tag{5}$$

It can be clearly seen from (1) that the synthesized reference signal is heavily dependent on $\hat{y}(n)$. In contrast, there is no such dependence on the feedforward ANC system, where the reference signal is obtained from the reference sensor. We shall analyze the effects of $\hat{y}(n)$ on the system behavior in following sections.

Therefore, in feedback ANC, there are two feedback loops, namely, the controller loop and the adaptive algorithm loop. The function of the controller loop is to synthesize the reference signal, while that of the adaptive algorithm loop is to adaptively generate the anti-noise. Due to the fact that there is high dependency between these loops, the computational analysis of the feedback ANC becomes complicated. Previous analyses have mainly focused on using frequency domain analysis, stochastic analysis, steady-state update analysis all under perfect secondary-path estimation assumption.

This paper attempts to give a quick overview of some preliminary analytical and simulation results of the convergence performance of the feedback ANC under imperfect secondary path estimation to cancel out narrowband noise. A more detailed report will be presented in [7]. The remaining of this paper is organized as follows. The next section presents the convergence analysis of the feedback ANC system. Section III outlines the estimation errors contributed by filtered-x and filtered-y signal paths in the feedback ANC system. Finally, Section IV concludes with the main findings of this paper.

II. Convergence Analysis of Feedback ANC System

The signal flow diagram of the feedback ANC system can be derived as shown in Fig. 3. The adaptive filter transfer function is based on the theoretical analysis proposed by Glover [8], which described the adaptive filter as a linear time-invariant system between the primary signal and error signal. Therefore, we can study the system stability property by examining the locations of poles in the system transfer function. In this study, we remove the assumption that the secondary path is always perfectly modeled. Instead, we assume that the synthesized reference signal consists of the reference signal and a periodic synthesized error signal as shown as

$$\begin{aligned} x_k(n) &= \hat{d}_k(n) \\ &= A\cos(\omega_0 n + \theta_k) + V\cos(\omega_0 n + \theta_v) \\ &= \frac{A}{2}(e^{j\omega_0 n}e^{j\theta_k} + e^{-j\omega_0 n}e^{-j\theta_k}) + \frac{V}{2}(e^{j\omega_0 n}e^{j\theta_v} + e^{-j\omega_0 n}e^{-j\theta_v}), \end{aligned} \tag{6}$$

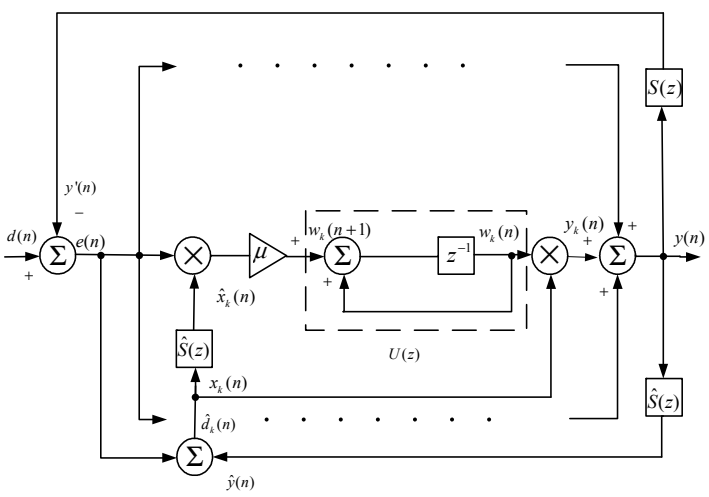

Figure 3. Signal flow diagram of the feedback ANC system using the FXLMS algorithm.

where ω_0 is the frequency of the narrowband noise, θ_v is the phase of the reconstruction error, k and n are the coefficient and time indices, respectively, A is the amplitude of the sinusoidal and V is the amplitude of the reconstruction error. The updating equation for individual weight coefficient can be expressed in the z-domain as

$$\begin{aligned} W_k(z) = {} & \frac{A}{2}\mu[\hat{S}(e^{j\omega_0})e^{j\theta_k}E(ze^{-j\omega_0}) + \hat{S}(e^{-j\omega_0})e^{-j\theta_k}E(ze^{j\omega_0})]U(z) \\ & + \frac{V}{2}\mu[\hat{S}(e^{j\omega_0})e^{j\theta_k}E(ze^{-j\omega_0}) + \hat{S}(e^{-j\omega_0})e^{-j\theta_k}E(ze^{j\omega_0})]U(z), \end{aligned} \tag{7}$$

where $\hat{S}(e^{j\omega_0})$ is the estimated secondary-path at the reference frequency, μ is the step size and $U(z) = \frac{1}{z-1}$ represents the iterative update of the adaptive filter weight. The contribution from the *k*th adaptive weight to the partial filter output $Y_k(z)$ can be expressed using the *z*-transform as

$$\begin{aligned} Y_k(z) &= Z\{w_k(n)x_k(n)\} \\ &= \frac{A}{2}e^{j\theta_k}W_k(ze^{-j\omega_0}) + \frac{A}{2}e^{-j\theta_k}W_k(ze^{j\omega_0}) \\ &\quad + \frac{V}{2}e^{j\theta_v}W_k(ze^{-j\omega_0}) + \frac{V}{2}e^{-j\theta_v}W_k(ze^{j\omega_0}). \end{aligned} \tag{8}$$

The four terms on the RHS of (8) are contributed form different signal paths and are either time invariant or time varying. We will define them as follows. The first and second terms on the RHS of (8) are both time-invariant terms contributed from the desired signal and the reconstructed error signal, respectively, and are denoted as TID and TIE. The third and forth terms are time varying contributed from the desired signal (TVD) and reconstruction signal (TVE), respectively. By combining the contribution from all partial filter outputs and convoluting with the actual secondary path transfer function, a secondary (or anti-noise) signal can be obtained:

$$
\begin{aligned}
Y'(z) &= S(z)\sum_{k=0}^{L-1} Y_k(z) \\
&= \frac{\mu L}{4}[\, A^2\hat{S}(e^{-j\omega_0})U(ze^{-j\omega_0}) + A^2\hat{S}(e^{j\omega_0})U(ze^{j\omega_0}) \\
&\quad + V^2\,\hat{S}(e^{-j\omega_0})U(ze^{-j\omega_0}) + V^2\,\hat{S}(e^{j\omega_0})U(ze^{j\omega_0})]S(z)E(z) \\
&\quad + \text{TVDs} + \text{TVEs}.
\end{aligned} \tag{9}
$$

The time varying terms can be neglected if we use a reasonably large filter length (L>8) is used. Therefore, the open-loop transfer function between $E(z)$ and $Y'(z)$ can be modeled by a linear, time-invariant system defined as

$$
\begin{aligned}
G(z) &= \frac{Y'(z)}{E(z)}. \\
&= \frac{\mu L}{4}[\, A^2\hat{S}(e^{-j\omega_0})U(ze^{-j\omega_0}) + A^2\hat{S}(e^{j\omega_0})U(ze^{j\omega_0}) \\
&\quad + V^2\,\hat{S}(e^{-j\omega_0})U(ze^{-j\omega_0}) + V^2\,\hat{S}(e^{j\omega_0})U(ze^{j\omega_0})]S(z) \\
&= \frac{\mu L}{4}[\, (A^2+V^2)\hat{S}(e^{-j\omega_0})U(ze^{-j\omega_0}) \\
&\quad + (A^2+V^2)\hat{S}(e^{j\omega_0})U(ze^{j\omega_0})]S(z).
\end{aligned} \tag{10}
$$

Equation (10) can be further simplified as:

$$
G(z) = \mu L\frac{(A^2+V^2)}{2}|\hat{S}|\frac{z\cos(\omega_0-\hat{\phi}_{\omega_0})-\cos\hat{\phi}_{\omega_0}}{z^2-2z\cos\omega_0+1}S(z) \tag{11}
$$

By inserting magnitude and phase errors into (11), we can expressed the open-loop transfer function as

$$
G(z) = \mu L|\hat{S}||S|\frac{(A^2+V^2)}{2}\left\{\frac{z\cos[\omega_0(\hat{\Delta}+1)]-\cos(\hat{\Delta}\omega_0)}{z^{\Delta}(z^2-2z\cos\omega_0+1)}\right\}. \tag{12}
$$

Substituting $V(z) = X(z)\left(1-\frac{\hat{S}(z)}{S(z)}\right)$ into (12), and expressing the closed-loop transfer function $H(z) = 1/(1+ G(z))$ and assuming $A = 1$, the closed-loop transfer function if the narrowband feedback ANC is expressed as

$$
H(z) = \frac{2|S|(z^2-2z\cos\omega_0+1)z^{\Delta}}{2|S|(z^2-2z\cos\omega_0+1)z^{\Delta}+\mu L(2|S|^2+|\hat{S}|^2\,z^{2\hat{\Delta}}-2|S||\hat{S}|z^{\Delta\hat{\Delta}})|\hat{S}|[z\cos(\omega_0(\hat{\Delta}+1))-\cos(\omega_0\hat{\Delta})]}. \tag{13}
$$

III. Estimation Errors Contribution

In this section, we look into the effects of the secondary-path estimation error on the step-size bounds of the feedback ANC system. We first examine the closed-loop transfer function under perfect secondary-path estimation and follows by imperfect secondary-path estimation.

Note that under perfect secondary-path estimation, the convergence condition for the feedback ANC system is the same as the feedforward ANC system. In [9], under perfect secondary-path estimation and for a sinusoidal reference signal, the step size bound is given by

$$
\mu < \frac{2}{(2\Delta+1)LP_{x'}}. \tag{14}
$$

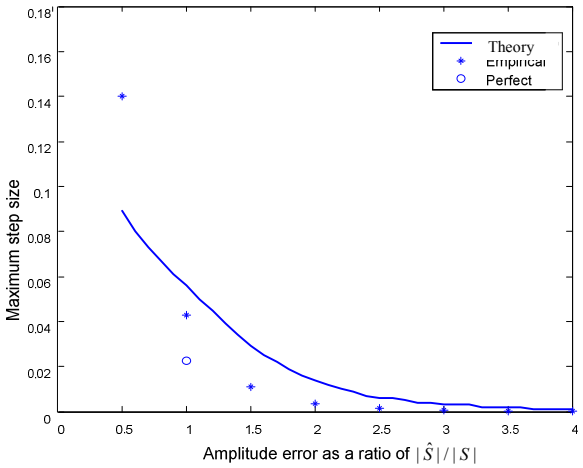

Figure 4: Maximum step size with imperfect secondary-path amplitude estimation error

In more recent studies reported in [10-11], an upper bound is obtained with a more general condition for feedforward ANC system., and arrives at the same step-size bound as in (14). Based on the closed-loop transfer function in (13) and under perfect secondary estimation, we can express (13) as

$$
H(z) = \frac{D(z)}{D(z)+\mu LN(z)}, \tag{15}
$$

where $D(z) = 2|S|(z^2-2z\cos\omega_0+1)z^{\Delta}$ and $N(z) = (2|S|^2+|\hat{S}|^2\,z^{2(\Delta-\hat{\Delta})}-2|S||\hat{S}|z^{\Delta-\hat{\Delta}})|\hat{S}|[z\cos(\omega_0(\hat{\Delta}+1))-\cos(\omega_0\hat{\Delta})]$.

According to [9], the upper bound of the step size can be found when $\omega_0 \to 0$ and $z \to 1$. As a result, we have

$$
\begin{aligned}
\mu_{\max} &= \frac{1}{L}\lim_{\omega_0\to 0, z\to 1}\left(-\frac{D(z)}{N(z)}\right) \\
&= \frac{4|\hat{S}|(|S|^2+|\hat{S}|-|S||\hat{S}|)}{(2\Delta+1)L}.
\end{aligned} \tag{16}
$$

The upper step size bound of the narrowband ANC is more accurate for lower frequency, which is suitable for active noise control applications that usually operate at frequency below 500 Hz. Furthermore, we can easily reduce (16) to (14) under perfect secondary path estimation and with an input power of 0.5.

In the case of imperfect secondary-path estimation, we can examine the maximum step-size bound due to amplitude error based on both theoretical and empirical results. Figure 4 shows the maximum step size bound with different amplitude estimation error. The theoretical result (represented as thick line) is close to the empirical results (represented as * symbol). As the estimation amplitude error is greater than the actual secondary path, the maximum step size bound is increased, and vice versa. This observation also coincide with that reported in [11] for the feedforward case.

In the case of estimation error deal to phase delay of the estimated secondary path, The estimation of the delay varies from 1 to 50 unit samples and the amplitude of the secondary-path estimation is perfect. The theoretical maximum step size bound is obtained by solving the characteristic equation of (16) and it is represented as solid line in Figure 5, while the empirical results are plotted as (*). The circle indicates perfect phase matching. The shaded area indicates the phase error exceeds the $\pm 90°$ phase error rule. The theoretical results correspond to the $\pm 90°$ bound stated in [2]. It is also observed that the maximum step size bound reduces

with increasing delay error. For the same phase error difference, a longer delay estimation further reduces the maximum step size. The relationship between the phase and delay errors with different sampling frequencies can be expressed as:

$$\Delta - \frac{f_s}{f_0} \times (k + 0.25) < \hat{\Delta} < \Delta + \frac{f_s}{f_0} \times (k + 0.25), \qquad (17)$$

where k is any integer that satisfies $k \le \text{int}\left(\frac{\Delta f_0}{f_s} - 0.25 \right)$.

IV. Conclusions

In this paper, the theoretical analysis of the step-size bound was formulated and verified through computer simulations for the narrowband feedback active noise control system under both perfect and imperfect secondary-path estimation. This preliminary result provides a mean to estimate the convergence analysis in a practical setting, where the secondary path estimation cannot be perfectly and continuously modeled in actual operation. To further quantify the effect of the filtered-x and filtered-y signal paths of the feedback active noise control system, [7] provides a more in depth examination of these signal paths and how they individually affect the convergence performance of the feedback active noise control.

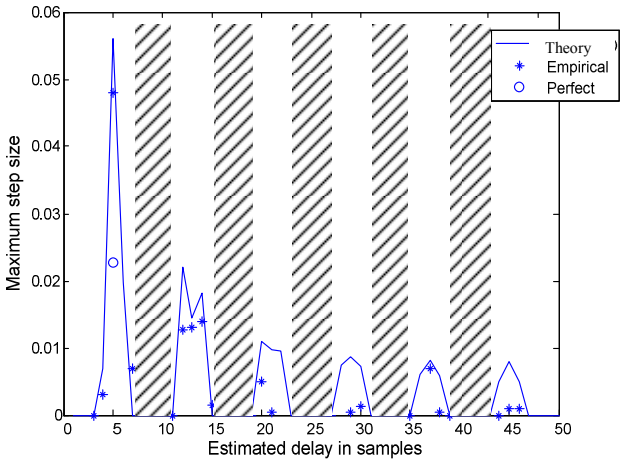

Figure 5: Maximum step size for different estimated delay for the imperfect secondary-path with reference to the actual secondary path.

Acknowledgment

This work is supported by the Singapore Ministry of Education Academic Research Fund Tier-2, under research grant MOE2010-T2-2-040.

References

[1] Y. Kajikawa, *W.S.Gan*, S.M. Kuo, "Recent Advances on Active Noise Control: Open Issues and Innovative Applications," in the inauguration issue of *APSIPA Transaction on Signal and Information Processing* (*Invited paper*), 2012.

[2] S. M. Kuo and D. R. Morgan, *Active Noise Control Systems—Algorithms and DSP Implementations,* New York: Wiley, 1996.

[3] P. A. Nelson and S. J. Elliott, *Active Control of Sound,* San Diego, CA: Academic, 1992.

[4] B. Widrow and S. D. Stearns, *Adaptive Signal Processing*. Englewood Cliffs, NJ: Prentice-Hall, 1985.

[5] H. Sakai and S. Miyagi, "Analysis of the adaptive filter algorithm for feedback-type active noise control," *Signal Processing*, vol. 83, no. 6, pp. 1291-1298, 2003.

[6] L. Wang, W. S. Gan, "Convergence analysis of narrowband active noise equalizer system under imperfect secondary path estimation," *IEEE Trans. Audio, Speech and Language Processing*, vol. 17, no. 4, pp. 566-571, May 2009.

[7] L. Wang et al., "Convergence Analysis of Narrowband Feedback Active Noise Control System with Imperfect Secondary-Path Estimation," submitted and under second round revision in *IEEE Trans. Audio, Speech and Language Processing.*

[8] J. R. Glover, "Adaptive noise cancelling applied to sinusoidal interferences," *IEEE Trans. Acoust., Speech, Signal Processing*, vol. 25, no. 6, pp. 484–491, Dec. 1977.

[9] E. Bjarnason, "Analysis of the Filtered-X LMS Algorithm," *IEEE Trans. Speech and Audio Processing*, vol. 3, no. 6, pp. 504–514, Nov. 1995.

[10] I. T. Ardekani and W. H. Abdulla, "On the stability of adaptation process in active noise control systems", *Journal of the Acoustical Society of America*, vol. 129, no. 1, 2011.

[11] I. T. Ardekani and W. H. Abdulla, "Effects of imperfect secondary path modeling on adaptive active noise control systems", *IEEE Trans. Control Systems Technology*, vol. 20, no. 5, pp. 1252-1262, Sep. 2012.